Journal of Manufacturing Engineering, June, 2013, Vol. 8, Issue. 2, pp 127-138

COMPLIANCE MODELING AND INTELLIGENT OPTIMIZATION OF KERF DURING WEDM OF AL7075/SiCP METAL MATRIX COMPOSITE

*** Thella Babu Rao[1] and Gopala Krishna A[2]**

[1]Department of Mechanical Engineering, GITAM University- Hyderabad Campus, Hyderabad, PIN - 502 329, Andhra Pradesh, India.
[2]Department of Mechanical Engineering, University College of Engineering, Jawaharlal Nehru Technological University, Kakinada, Andhra Pradesh, PIN - 533 003, India.

ABSTRACT

This investigation presents the formulation of the kerf (width of the slit) and the optimal control parameter settings of wire electrochemical discharge machining (WEDM) for machining Al7075/SiC_P MMCs. WEDM has proven its economical efficiency and effectiveness in cutting the hard ceramic reinforced MMCs. Kerf is an important performance characteristic which determines the dimensional accuracy of the machined component while producing high precision components. Lack of availability of machinability information for advanced MMCs necessitates more experimental trials in manufacturing industry. Therefore, extensive experimental investigations are essential to predict kerf. This work is aimed to investigate the significance of particulate size, volume fraction of SiC_P, pulse-on time, pulse-off time and wire tension on the kerf. A response surface model was developed to predict and analyze the relative significance of the control variables on kerf and was confirmed for its adequacy by several statistical tests. A powerful artificial intelligence called genetic algorithms (GA) was then used to determine the best combination of the control variable settings. In the next step the derived optimal settings were confirmed by experimental validation. The results obtained in this work state that, the derived optimized parameters are capable of machining the Al7075/SiC_P MMCs more efficiently and with better dimensional accuracy.

Keywords: *Al7075/SiC_P MMCs, kerf, WEDM and Optimization.*

1. Introduction

Metal matrix composites have found diverse applications in the present aerospace and automobile industries. These are classified as advanced materials due to their improved properties of high strength-to-weight ratio, excellent wear resistance, lower coefficient of thermal expansion and capability to work at elevated temperatures [1].

MMCs are manufactured using several methods such as powder metallurgy, uni-axial pressing, iso-static pressing, extrusion, spray forming, stir-casting, rheo-casting and compo-casting. However, the presence of discontinuously dispersed hard ceramic results in poor machinability poses a challenge to the manufacturing industry today. As a result the application of such materials has been restricted to only a limited variety of components. The factors like chemical composition, ceramic reinforcement and its distribution, processing rout and the processing conditions are highly significant to the machinability of MMCs. The conventional machining methods like turning, milling, drilling are found uneconomical due to the severe tool wear resulting from the presence of hard ceramic content [2, 3].

However, the non-conventional machining methods like laser beam machining (LBM), plasma cutting, and electron beam machining (EBM) are being used in the industries to cut these composites, but are identified as highly expensive requiring huge and costly equipment in their operation. On the other hand, electric discharge machining (EDM) has become a popular method for its efficiency and cost effectiveness to machine these composites. However it is limited to producing simple contours on the machined part. It also requires elaborate preparation for pre-shaped electrode as a tool to get the required contours over the component. Subsequently, Wire electrical discharge machining (WEDM) as a non-contact type machining method has proved to be an economical and efficient method for machining metal matrix composites into complex contours [4, 5]. In its working principle, WEDM is a thermo-electrical process in which the metal removal takes place in a series of discharges of electric sparks at the interface of continuously supplied and directed wire (electrode) and the workpiece in the presence of dielectric medium. Control parameters like discharge current, pulse-on time, pulse-off time, and

**Corresponding Author - E- mail: baburao_thella@yahoo.co.in*

voltage are the most common significant factors for high speed machining of WEDM [6, 7], while in the case of machining metal matrix composites, variables like volume fraction and particulate size have considerable effect on the performance of the WEDM.

Table 1: Machining conditions

S. No.	Description
1	Work piece (anode) : Al7075/SiCp
2	Tool (cathode) : Brass wire, diameter 250 μm
3	Work piece height: 6 mm
4	Cutting length: 75 mm.
5	Angle of Cut: Vertical
6	Location of work piece : centre to the table
7	Servo reference voltage : 35V
8	Average voltage gap maintained: 40V
9	Die-electric temperature: 25°C
10	Die-electric fluid: Distilled water

Usually, manufacturers of WEDM machines provide the database of electrode materials and the operational details and process control variables for most regularly used materials only. The information provided by the manufactures of WEDM is not adequate for machining MMCs. Hence, the database of feasible control variables of WEDM for machining MMCs could widen their applications in industries. One of the most significant performance characteristics of the WEDM process is kerf. The kerf determines the dimensional accuracy of the machined component. According to Aniza et al. [8] increased feed rate increases kerf but also causes by inaccuracies in the kerf [9]. Sangju Lee et al. [10] found that the reason for decreased kerf at higher feed rate. This is due to less lateral discharge energy. Electrical parameters like voltage and pulse duration are highly significant factors for kerf [11]. Therefore, an extensive experimental work is needed to completely understand the individual and interactive effects of various WEDM control parameters.

This investigation is aimed to provide the empirical model to predict the kerf in terms of the most significant WEDM control parameters for Al7075/SiC_p MMC using response surface methodology (RSM) and to find the optimal control variables which machine the composite with minimum possible kerf using genetic algorithms (GA).

Table 2: Control factors and their levels

S.No.	Variable		Levels		
			1	**2**	**3**
1	Particulate size (μm)	X_1	25	50	75
2	Volume of SiC_P (%)	X_2	5	10	15
3	Pulse-on Time (μs)	X_3	5	8	9
4	Pulse-off Time (μs)	X_4	25	35	45
5	Wire Tension (gms)	X_5	1	5	9

Table 3: Design of experimental matrix: Taguchi's L_{27} orthogonal array

Exp. No.	Coded control factor					Kerf (mm)
	X_1	X_2	X_3	X_4	X_5	
1	1	1	1	1	1	0.305
2	1	1	2	2	2	0.359
3	1	1	3	3	3	0.389
4	1	2	1	2	2	0.311
5	1	2	2	3	3	0.341
6	1	2	3	1	1	0.347
7	1	3	1	3	3	0.301
8	1	3	2	1	1	0.324
9	1	3	3	2	2	0.341
10	2	1	1	2	3	0.331
11	2	1	2	3	1	0.338
12	2	1	3	1	2	0.362
13	2	2	1	3	1	0.282
14	2	2	2	1	2	0.331
15	2	2	3	2	3	0.343
16	2	3	1	1	2	0.311
17	2	3	2	2	3	0.318
18	2	3	3	3	1	0.318
19	3	1	1	3	2	0.304
20	3	1	2	1	3	0.331
21	3	1	3	2	1	0.334
22	3	2	1	1	3	0.312
23	3	2	2	2	1	0.314
24	3	2	3	3	2	0.323
25	3	3	1	2	1	0.285
26	3	3	2	3	2	0.300
27	3	3	3	1	3	0.325

2. Experimental Procedures

A robust Taguchi's design of experiments (DOE) is employed to minimize the number of experimental runs and the experiments are designed for an L_{27} orthogonal array consisting of 27 experimental runs [12]. Then the machining was conducted on a five-axis CNC-Wire Electrical Discharge Machine, Model Number CT 520A, made by Joemars Machinery and

Electric Industrial Co.Ltd., Taiwan. SiC_P reinforced Al7075 metal matrix composites are used as work pieces for machining. These MMCs are produced by stir casting. The MMCs are produced with different particulate sizes of 25, 50 and 75µm reinforced each at distinct volume fractions as 5, 10 and 15%.

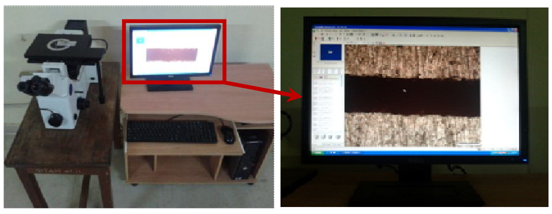

Fig. 1 Experimental setup for Kerf measurement

The details of work specimens, the electrode and the other machining conditions are listed in Table 1. Pulse-on time, pulse-off time and wire tension were selected as WEDM process parameters in addition to the composite variables of particulate size and volume fraction of SiC_p. The levels of process variables were selected based on the literature and the pilot experiment as listed Table 2. The design of experimental matrix is listed in Table 3.

After each experiment, kerf of the machined work piece was measured by using Computerized Optical Microscope, model GX51 inverted microscope made by OLYMPUS CORPORATION with the magnification range of 200µm. These were measured at six different locations along the machined length in a perpendicular direction and the averages of them were considered the kerf and are listed in Table 3.

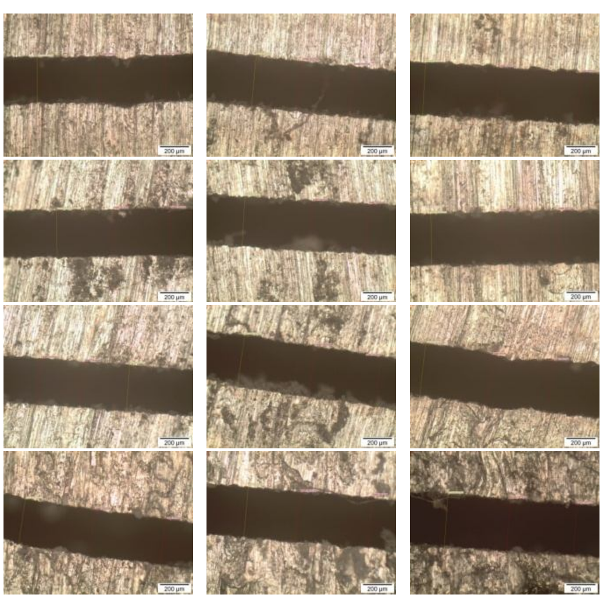

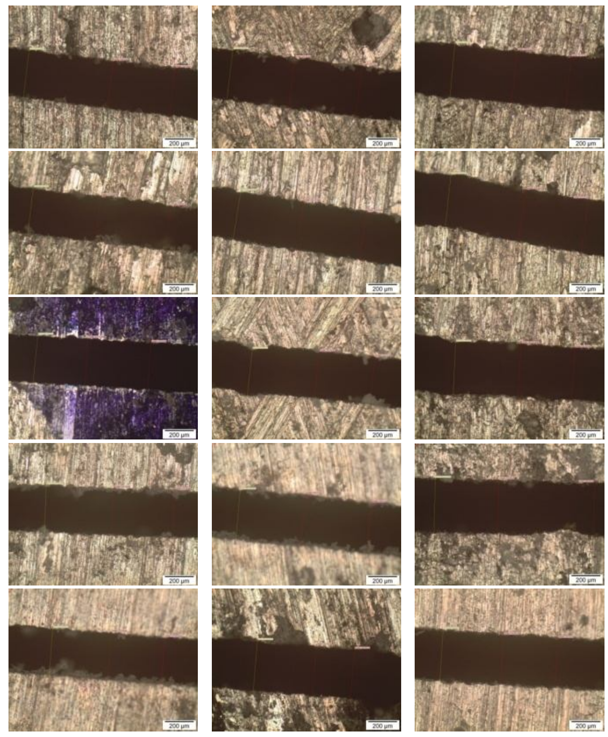

Fig. 2 Measurement of Kerf for 27 experiments

Fig. 1 shows the experimental setup used to measure the response kerf and the Fig. 2 represents the kerf width of the machined composites.

3. Postulation of Model

The experimental measurements at each run were used to develop the mathematical model based on response surface methodology. This model relates the considered kerf with various control variable settings during machining Al7075/SiC_P. WEDM is such a complex process that interaction effects of the control variables are highly significant for machining performances. Therefore the second order polynomial models were fitted for the output responses in terms of the coded variables. The postulated model is represented in terms of regression coefficients as follows:

$$\begin{aligned} \mathrm{Kw} = {} & 0.33 - 0.0099x_1 - 0.013x_2 + 0.019x_3 - 0.0042x_4 \\ & +0.0064x_5 - 0.0019x_1{}^2 + 0.0038x_2{}^2 - 0.0049x_3{}^2 \\ & +0.0002x_4{}^2 - 0.0036x_5{}^2 + 0.0047x_1x_2 - 0.0041x_1x_3 \\ & -0.0029x_1x_4 - 0.0024x_1x_5 - 0.0026x_2x_3 - 0.0065x_2x_4 \\ & -0.0025x_2x_5 + 0.0009x_3x_4 - 0.0053x_3x_5 + 0.0012x_4x_5 \end{aligned} \quad (1)$$

In the above equation x_1, x_2, x_3, x_4 and x_5 represent the logarithmic transformations for the control factors, particulate size, volume of particulate, pulse-on time, pulse-off time and wire tension respectively and they are given below:

$$x_1 = \frac{\ln(X_1) - \ln(50)}{\ln(75) - \ln(50)};\ x_2 = \frac{\ln(X_2) - \ln(10)}{\ln(15) - \ln(10)};$$
$$x_3 = \frac{\ln(X_3) - \ln(7)}{\ln(9) - \ln(7)};x_4 = \frac{\ln(X_4) - \ln(35)}{\ln(45) - \ln(35)}; \quad (2)$$
$$x_5 = \frac{\ln(X_5) - \ln(5)}{\ln(9) - \ln(5)}$$

The above transformations are obtained by the following formula:

$$x = \frac{\ln(X_n) - \ln(X_{n0})}{\ln(X_{n1}) - \ln(X_{n0})} \quad (3)$$

Where x is the coded value of any factor corresponding to its natural value X_n; X_{n1} is the natural value of the factor of the + level, and X_{n0} is the natural value of the factor corresponding to the base level or zero level.

4. Analysis of Variance

The developed empirical model was confirmed for its adequacy using the following tests. Firstly, analysis of variance (ANOVA) was carried out for the quadratic response surface model and its statistics are given in the Tables 4. It can be observed from Table 4 that the value of "Prob. > F" for the model is less than 0.05, which indicates that the model is significant [13]. In the second, the multiple regression coefficient (R^2) is computed to check whether the fitted models actually describe the experimental data. R^2 is defined as the ratio of variability explained by the model to the total variability in the actual experimental data and is used as a measure of goodness of fit [13]. If R^2 approaches to unity, the model fits the experimental data better. In other words, it is the proportion of variation in the dependent variable (response) that can be explained by the predictors (factor) in the model. From Table 4, R^2 for kerf is found to be 0.9938. This shows that the second-order model can explain the variation in kerf up to the extent of 99.38%.

From Table 4, adjusted R^2 for kerf is found to be 0.9770. It can be observed that the values of R^2 and adjusted R^2 are much closer to each other. This proves that the developed model represents the process adequately. Thus, the developed mathematical model was checked for its adequacy using a normal probability plot of residuals. The diagnostic plots were drawn to check whether the data was normally distributed and whether any assumption was violated. In a normal probability plot, if all the data points fall near the line, an assumption of normality is reasonable. Otherwise, the points will curve away from the line, and an assumption of normality is not justified [13]. The normal probability plot of the residuals for the output response, kerf is shown in Fig. 3 and it can be observed that the residuals are located on a straight line, which means that the errors are distributed normally.

Table 4: ANOVA [Partial sum of squares] for kerf

Source	**Sum of squares**	**d. f.**	**Mean square**	**F-value**	**Prob. > F**
Model	0.014484	20	0.000724	48.309	<0.0001
X_1	0.000614	1	0.000614	40.924	<0.0007
X_2	0.002939	1	0.002939	196.04	<0.0001
X_3	0.004548	1	0.004548	303.37	<0.0001
X_4	9.05E-05	1	9.05E-05	6.034	<0.0494
X_5	0.000224	1	0.000224	14.942	<0.0083
X_1X_2	0.000152	1	0.000152	10.125	<0.0190
X_1X_3	7.51E-05	1	7.51E-05	5.006	0.0666
X_1X_4	1.25E-05	1	1.25E-05	0.834	0.3962
X_1X_5	1.11E-05	1	1.11E-05	0.743	0.4216
X_2X_3	4.35E-05	1	4.35E-05	2.898	0.1396
X_2X_4	0.000406	1	0.000406	27.08	<0.0020
X_2X_5	4.35E-05	1	4.35E-05	2.900	0.1394
X_3X_4	6.24E-06	1	6.24E-06	0.416	0.5427
X_3X_5	0.000172	1	0.000172	11.44	<0.0148
X_4X_5	2.9E-06	1	2.9E-06	0.193	0.6754
X_1X_1	1.27E-05	1	1.27E-05	0.848	0.3924
X_2X_2	8.38E-05	1	8.38E-05	5.593	0.0559
X_3X_3	0.000143	1	0.000143	9.564	0.0213
X_4X_4	3.86E-08	1	3.86E-08	0.002	0.9612
X_5X_5	2.38E-05	1	2.38E-05	1.590	0.2541
Res.	9.0E-005	7	1.287E-5		
Pure Error	5.5E-006	5	1.1E-006		
Cor Total	0.015	26			
St.dev.	3.59E-03			R^2	0.9938
Mean	0.33			Adj. R^2	0.9733

< - refers to significant terms

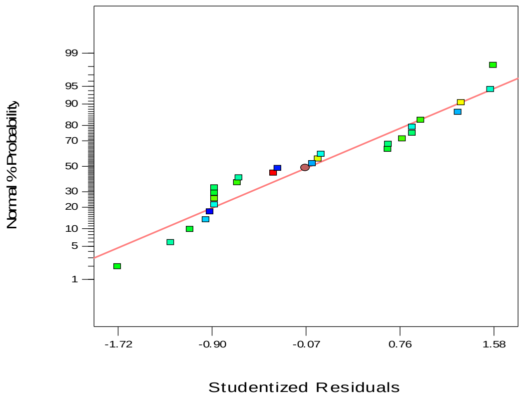

Fig. 3 Normal probability plot of residuals for kerf

5. Influence of Control Variables

From Table 4, it can be observed that the main effects of particulate size (X_1), the percentage of the reinforcement (X_2), pulse-on time (X_3), pulse-off time (X_4) and wire tension (X_5) are significant on Kerf. Also, the interactive effects of particulate size and percentage of the reinforcement (X_1X_2), percentage of the reinforcement and pulse-off time (X_2X_4), and pulse-on time - wire tension (X_3X_5) are significant.

From Fig. 4 and 5, it is observed that the combined effect of increased particulate size and fraction of the particulate is considerably decreasing the kerf, due to the increased hardness of the material resulting from compacted and large particulate in the matrix. Fig. 6, shows that, the kerf is greatly affected by the pulse-on time. It is obvious that the increased electric discharge energy causes deeper and wider craters which widen the gap between the wire and the work piece. Fig. 7 shows that, the kerf is also affected by the pulse-off time but is in negative compared to pulse-on time. Fig. 8 depicts the significance of wire tension on the Kerf. The increasing trend of the Kerf can be observed with increased wire tension due to the stabilized arc between the work piece and the tensed wire.

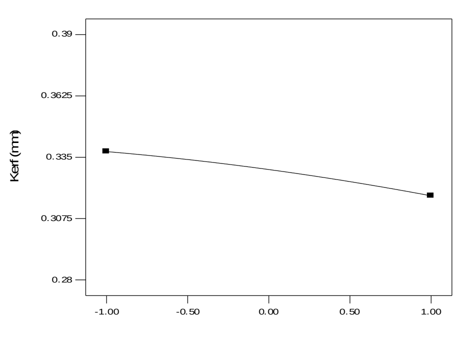

Fig. 4 Effect of particulate size on kerf

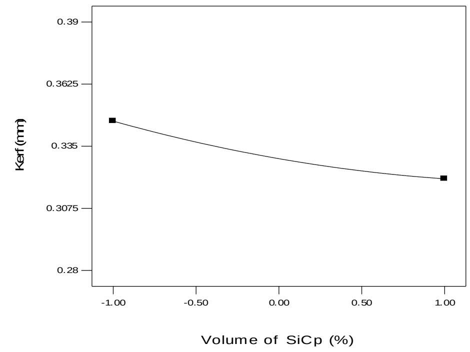

Fig. 5 Effect of volume fraction of SiC$_P$ on kerf

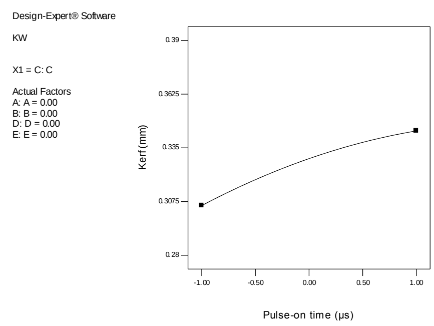

Fig. 6 Effect of pulse-on time on kerf

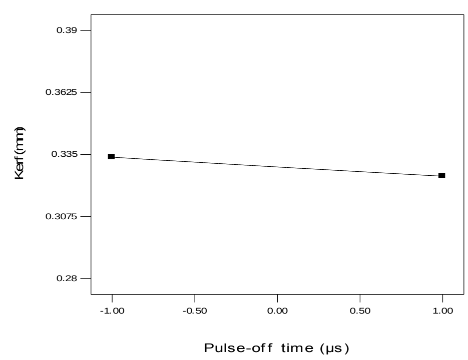

Fig. 7 Effect of pulse-off time on kerf

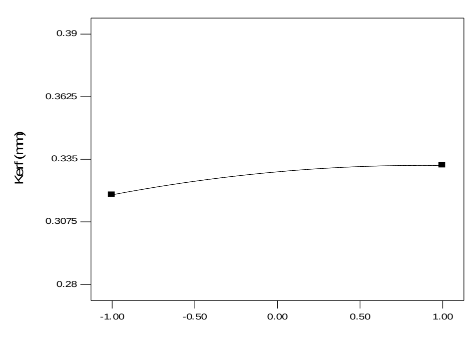

Fig. 8 Effect of wire tension on kerf

Fig. 9 presents the interactive effects of particulate size and percentage of the reinforcement on Kerf. The presence of hard SiC_P on the cutting path and the increased hardness due to the increased size and addition of particulate are the reasons for decreasing the kerf. From Fig. 10, it is obvious that higher volume of reinforcement in combination with increased pulse-off time reduces the kerf. However, the combined effect of increased pulse-on time and wire tension causes increase of the Kerf greatly as shown in the Fig. 11.

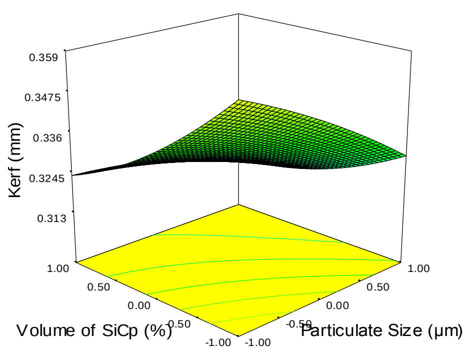

Fig. 9 Interactive effect of particulate size and volume fraction of SiC_P on kerf

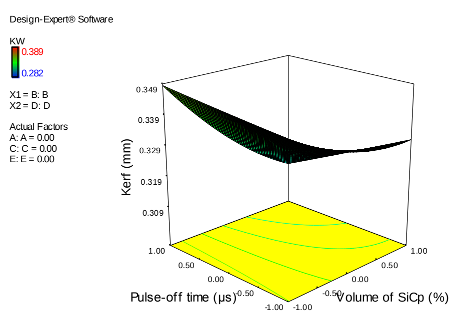

Fig. 10 Interactive effect of volume fraction of SiC_P and pulse-off time on kerf

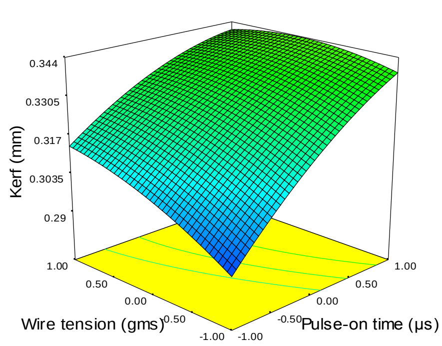

Fig. 11 Interactive effect of pulse-on time and wire tension on kerf

6. Formulation Of Optimization Problem

In order to optimize the measured response, the problem is formulated as a single objective optimization problem of minimization of kerf subjected to the boundaries of the variables varied in the machining experiments. The problem is formulated as follows:

To find: X_1, X_2, X_3, X_4 and X_5 (4)

Minimize:

$$\begin{aligned} Kw &= 0.33 - 0.0099x_1 - 0.013x_2 + 0.019x_3 - 0.0042x_4 \\ &+ 0.0064x_5 - 0.0019x_1^2 + 0.0038x_2^2 - 0.0049x_3^2 \\ &+ 0.0002x_4^2 - 0.0036x_5^2 + 0.0047x_1x_2 - 0.0041x_1x_3 \\ &- 0.0029x_1x_4 - 0.0024x_1x_5 - 0.0026x_2x_3 - 0.0065x_2x_4 \\ &- 0.0025x_2x_5 + 0.0009x_3x_4 - 0.0053x_3x_5 + 0.0012x_4x_5 \end{aligned} \tag{5}$$

Subjected to,

$25\ \mu m \le X_1 \le 75\ \mu m$ (6)

$5\ \% \le X_2 \le 10\ \%$ (7)

$5\ \mu s \le X_3 \le 9\ \mu s$ (8)

$25\ \mu s \le X_4 \le 45\ \mu s$ (9)

$1\ g \le X_5 \le 9\ g$ (10)

7. Optimization Using GA

Applying genetic algorithms is the ideal approach for the complex multi-variable optimization problems [14]. GA as a non-traditional optimization method is being successfully implemented in a variety of the manufacturing applications [15]. Palanisamy et al. [16] implemented GA to find the optimum machining parameters for end-milling operations. They highlighted the accuracy and effectiveness of GA based on the good agreement between GA results and the experimentally validated results of this investigation. The methodology of GA begins with the generation of a set of strings (or chromosomes) randomly called a population. Traditionally, a binary coding system is adopted to represent the chromosomes in terms of either zeros or ones. After the fitness value (objective function value) is computed for each member of the population, the three fundamental GA operators called reproduction, crossover and mutation are operated on the population to create a new population also called child population. The child population is further evaluated and tested for determination with reference to the parent population. In the simulation of GA, one iteration of these three operators is named as generation [17].

In this investigation, GA was implemented to the formulated objective function to find the global minimum value of the kerf. The implementation of GA is clearly explained in the Tables 5, 6 and 7 for minimizing the Kerf as objective. For one iteration of the algorithm, the sample calculations are presented here. The bit lengths of 5, 4, 4, 3 and 3 are chosen for X_1, X_2, X_3, X_4 and X_5 respectively. The initial population with 27 chromosomes is randomly generated as a first step of the algorithm and is shown in Table 5. The decoded decimal values of Kerf of the generated chromosome strings of individual input variables are listed in Table 5. For example, from Table 5, the first string (10011 1111 1101 000 111) is decoded to values equal to X_1=56; X_2=15; X_3=8; X_4=25; X_5=9 using linear mapping rule as presented in the eq.11.

$$x_i = X_i^L + \frac{X_i^U - X_i^L}{2^{l_i} - 1} \times decoded\ value \qquad (11)$$

Then the objective function Kerf value was computed and obtained as 0.3357. The fitness function value at this point using the transformation rule $F(x(1)) = \frac{1}{1+0.3357}$ was obtained as 0.7486. This fitness function value was used in the reproduction operation of the GA. Similarly, other strings in the population were evaluated and fitness values were calculated. Table 5 shows the objective function value and the fitness value for all the 27 strings in the initial population. In the next step, good strings in the population were to be selected to form the mating pool. In this work, roulette-wheel selection procedure was used to select the best strings. As a part of this procedure, the average fitness of the population was calculated by adding the fitness values of all strings and dividing the sum of the population size and the average fitness of the population $(\bar{F})$ was obtained as 0.7570.

The expected count was subsequently calculated by dividing each fitness value with the average fitness, $(F(x)/\bar{F})$. For the first string, the obtained expected count is (0.7486/0.7570) = 0.989. Similarly, the expected count values were calculated for all other strings in the population and shown in Table 6. Then, the probability of each string being copied in the mating pool can be computed by dividing the expected count values with the population size. For instance, the probability of the first string is (0.989/27) = 0.037. Similarly, the values of the probability of selection of all the strings were calculated and cumulative probability was henceforward computed. The probabilities of selection are listed in Table 6.

Now, random numbers between zero and one were generated in order to form the mating pool. From Table 6, random number generated for the first string is 0.225 which means the sixth string from the population gets a copy in the mating pool, because that string occupies the probability interval (0.222, 0.260) as shown in the column of cumulative probability in the Table 6. In a similar manner, the other strings were selected according to the random numbers generated in Table 7.16 and the complete mating pool was formed. The mating pool is displayed in Table 7. By adopting the reproduction operator, the inferior points were automatically eliminated from further consideration.

Table 5: Initial population with fitness values in GA

S. No.	Chromosomes	X_1	X_2	X_3	X_4	X_5	Kerf	Fitness value
1	10011 1111 1101 000 111	56	15	8	25	9	0.336	0.749
2	10111 1101 0011 011 000	62	14	6	34	1	0.299	0.770
3	11000 0100 1111 101 100	64	8	9	39	6	0.339	0.747
4	11001 0110 0101 000 001	65	9	6	25	2	0.313	0.762
5	10101 0010 1100 110 001	59	6	8	42	2	0.338	0.747
6	11010 1001 0010 000 010	67	11	6	25	3	0.305	0.766
7	11101 1011 0110 100 001	72	12	7	36	2	0.306	0.766
8	01111 1111 1000 001 101	49	15	7	28	7	0.328	0.753
9	10011 0000 1101 010 111	56	5	8	31	9	0.357	0.737
10	10001 1101 0011 110 011	52	14	6	42	4	0.298	0.770
11	10100 0110 0101 001 101	57	9	6	28	7	0.325	0.755
12	10011 0101 0101 010 010	56	8	6	31	3	0.318	0.759
13	10101 1101 0011 111 101	59	14	6	45	7	0.299	0.770
14	11111 0111 0001 000 111	75	10	5	25	9	0.312	0.762
15	11001 1100 1100 011 001	65	13	8	34	2	0.323	0.756
16	10011 1111 0011 010 101	56	15	6	31	7	0.313	0.762
17	11001 0011 1100 101 010	65	7	8	39	3	0.334	0.750
18	10101 1010 1010 000 111	59	12	8	25	9	0.335	0.749
19	01010 0101 1110 100 001	41	8	9	36	2	0.345	0.743
20	11000 1100 0011 111 001	64	13	6	45	2	0.291	0.775
21	11001 1011 1001 100 001	65	12	7	36	2	0.315	0.760
22	10001 1101 0110 001 110	52	14	7	28	8	0.326	0.754
23	11011 0101 0011 101 011	69	8	6	39	4	0.307	0.765
24	10011 1100 1011 011 011	56	13	8	34	4	0.325	0.755
25	00100 0010 0010 110 001	31	6	6	42	2	0.316	0.760
26	00011 0011 0110 001 010	30	7	7	28	3	0.336	0.749
27	11101 0110 1111 000 001	72	9	9	25	2	0.334	0.750

As a next step in the generation, the strings in the mating pool were used for the crossover operation. In the crossover operation, two strings were selected at random and crossed at a random site. Since the mating pool contains strings at random, pairs of strings were picked-up from the top of the list as shown in Table 7. Thus strings 6 and 20 participate in the first crossover operation. In this work, two-point crossover [18] was adopted with the probability, p_c=0.85 to check whether a crossover was desired or not. To perform a crossover, a random number was generated with crossover probability (p_c) of 0.85. If the random number was less than p_c then the crossover operation is performed, otherwise the strings are directly placed in an intermediate population for subsequent genetic operation. When a crossover is required to be performed then crossover sites are to be decided at random by creating random numbers between (0, *l*-1), where l represents the total length of the string. For example, when a crossover is required to be performed for the strings 24, 13 two sites of crossover are to be selected randomly. Here, the random sites happened to be 9, 16. Thus the portions between sites 9 and 16 of the strings 24 and 13 were swapped to create the new offspring as shown in Table 7.

However, with the random sites, the children strings produced may or may not have a combination of good strings of parent strings, depending on whether or not the crossing sites fall in the appropriate locations. If good strings are not created by crossover, they will not survive too long because reproduction will select against those chromosomes in subsequent generations. In order to preserve some of the best chromosomes that are already present in the mating pool, all the chromosomes are not used in crossover operation. When a crossover probability of p_c is used, the expected number of strings that will be subjected to crossover is only 100p_c and the remaining percent of the population remains as it is in the current population. The calculations of intermediate population are shown in the Table 7. The crossover is mainly responsible for the creation of new strings.

The third operator, mutation, was then applied to the intermediate population. Mutation is basically intended for local search around the current solution. Bit-wise mutation was performed with a probability, p_m=0. 10. A random number was generated with p_m; if the random number is less than p_m then the bit is altered from 1 to 0 or 0 to 1 depending on the bit value otherwise no action was taken. Mutation was implemented with the probability, p_m=0.10 as shown in Table 7. The procedure is repeated for all the strings in the intermediate population. This completes one iteration of the GA. The above procedure is continued until the maximum number of generations was completed. For better convergence, the algorithm was run for 500 generations.

8. Results and Discussion

In order to find the optimal machining parameters that result in the best global minimum value of Kerf, the MATLAB GA toolbox was used to simulate the algorithm. One of the major advantages with GA is that the users need not supply any supporting information excluding the objective function values and constraints. In addition, no assumptions are to be made while applying the algorithm and it works with a population of points instead of a single point. GA narrows down the search space as the search progresses.

Table 6: Selection in GA (Minimization of Kerf)

S. No.	Expected Count	Probability	Cumulative Probability	Random Number	Selected String Number
1	0.989	0.037	0.037	0.225	6
2	1.017	0.038	0.074	0.721	20
3	0.987	0.037	0.111	0.346	9
4	1.006	0.037	0.148	0.354	10
5	0.987	0.037	0.185	0.887	24
6	1.012	0.037	0.222	0.493	13
7	1.011	0.037	0.260	0.329	8
8	0.994	0.037	0.296	0.086	2
9	0.973	0.036	0.332	0.044	1
10	1.018	0.038	0.370	0.687	18
11	0.997	0.037	0.407	0.650	17
12	1.002	0.037	0.444	0.084	2
13	1.017	0.038	0.482	0.032	1
14	1.007	0.037	0.519	0.886	24
15	0.998	0.037	0.556	0.536	15
16	1.006	0.037	0.593	0.840	23
17	0.990	0.037	0.630	0.732	20
18	0.990	0.037	0.667	0.281	8
19	0.982	0.036	0.703	0.869	23
20	1.024	0.038	0.741	0.882	24
21	1.004	0.037	0.778	0.125	4
22	0.996	0.037	0.815	0.421	11
23	1.011	0.037	0.853	0.913	25
24	0.997	0.037	0.890	0.538	14
25	1.004	0.037	0.927	0.393	11
26	0.989	0.037	0.963	0.272	7
27	0.991	0.037	1.000	0.034	1

In the present problem, GA was run for 500 generations and the algorithm was converging to the objective function value of 0.272. The fitness value convergence graph is displayed in Fig. 12 and the optimal values of the control factors are listed in Table

8. The following results are resolved from the simulation results through the proposed methodology: From the experimental observations in Table 3 the least kerf value measured is 0.282 for the 13th experiment. However, after optimization using GA, it is observed from Table 8 that Kerf decreased to 0.276 mm. It means around 3.546% of the kerf value can be minimized by adopting the machining control variables listed in Table 8.

Table 8: Optimum machining conditions for Kerf

Control factors and Responses	Optimum value GA	Optimum value Experimental
Particulate size (μm)	65.84	65.00
%volume of SiC_P	14.32	14.32
Pulse-on time (μs)	5.00	5.00
Pulse-off time (μs)	44.85	44.85
Wire tension (gm)	1.00	1.00
Kerf (mm)	0.272	0.274

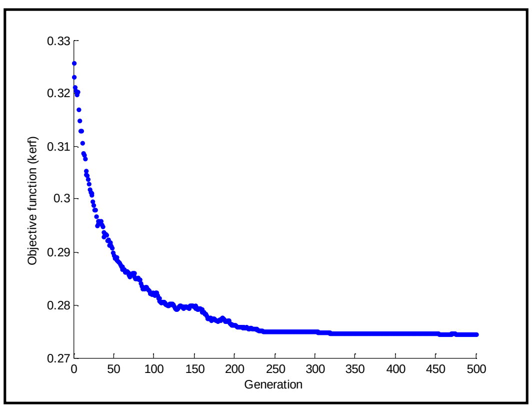

Fig. 12 Convergence graph for minimization of Kerf

9. Confirmation Experiments

The next step to the optimization is the experimental validation of the obtained results from the proposed method. Therefore, confirmation experiments were conducted to validate the predicated response surface model of the Kerf. The values of the control variables were selected within the upper and lower limit values used for experimentations in the design matrix and to derive the models.

The same experimental setup was used to conduct the validation tests in the manufacturing facility. A total of eighteen confirmation experiments were performed with distinct parameter settings and the measured Kerf values are listed in Table 9. A comparative study between the predicted and experimental results was carried out and furnished in Table 9.

Fig. 13 shows the one-to-one plots drawn between the predicted values and the experimental values. It is observed from the figures that the proposed methodology ensures reasonable predictions and it can be concluded that the developed mathematical models have good agreement with the experimental test lines. Slight variations between the results might be due to random factors like probable material defects and minute tool deflection from its mean position because of electrodynamic forces on the wire.

10. Conclusions

Precise machining of metal matrix composites is very much essential for the industries today. Wire electrical discharge machining proved as an efficient and economical non-traditional machining method to cut the hard ceramic reinforced MMCs. Optimization of WEDM control variables for machining the advanced MMCs is vital for improving the performance of the process. At the point of accurate machining, optimal settings of control variables play an important role in maintaining the closer dimensional tolerances of the machined component. As in the case of WEDM kerf represents the dimensional accuracy of the machining component, the investigation was directed to determine the optimal process parameters which can produce the best minimum possible kerf during WEDM of various SiC_P reinforced Al7075 MMCs.

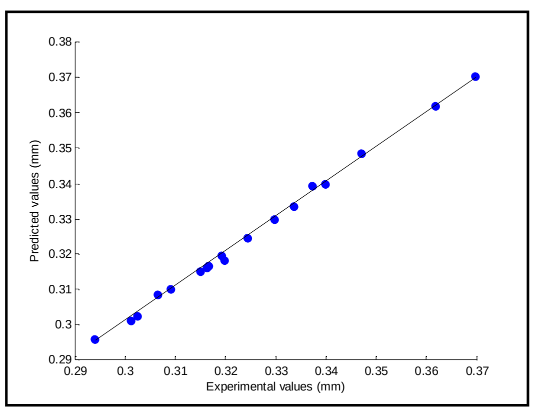

Fig. 13 Predicted values vs. experimental values for Kerf

The experimental runs were conducted on stir cast composites of Al7075/SiC_P having three distinct SiC particulate size viz., 25, 50 and 75 μm and were at 5, 10 and 15% by volume of the matrix. The experiments were designed based on the Taguchi's orthogonal array. During the experimentation, the most significant process parameters of the WEDM process of pulse-on time, pulse-off time and wire tension were used as machining variables along with the particulate size and volume fraction of the SiC_P in the workpiece to measure the kerf as the process response. Based on the experimental measurements, an empirical model was derived by using response surface methodology. The model facilitates predicting of the kerf in WEDM and helps in process optimization. Consequently, GA are used to determine the optimal parameters that reduced the kerf to 0.272 mm. Hence, GA-based optimization system developed to machine Al7075/SiC_P using WEDM would improve the machining efficiency by 3.546% using optimal cutting parameters. Also the proposed methodology could help to automate the machining system at the computer aided process planning (CAPP) stages to produce high quality components of Al7075/SiC_P MMCs with tight tolerances by WEDM.

Appendix A : Table 7 Crossover and Mutation in GA (Min. of Kerf)

Appendix B : Table 9 Validation of results for Kerf

References

1. *M. Rosso, Ceramic and metal matrix composites: Routes and properties, Journal of Materials Processing Technology 175 (2006) 364–375*

2. *A. Manna Æ B. Bhattacharyya, Investigation for optimal parametric combination for achieving better surface finish during turning of Al /SiC-MMC, Int J Adv Manuf Technol (2004) 23: 658–665.*

3. *Harlal Singh Mali, Alakesh Manna, Simulation of surface generated during abrasive flow finishing of Al/SiC p -MMC using neural networks, Int J Adv Manuf Technol (2012) 61:1263 – 1268.*

4. *Ho KH, Newman ST, Rahimifard S, Allen RD (2004) State of the art in wire electrical discharge machining (WEDM). Int J Mach Tools Manuf 44:1247 – 1259.*

5. *C. Satishkumar, M. Kanthababu, V. Vajjiravelu, R. Anburaj, N. Thirumalai Sundarrajan, H. Arul, Investigation of wire electrical discharge machining characteristics of Al6063/SiC p composites, Int J Adv Manuf Technol (2011) 56:975 – 986.*

6. *Guo ZN, Wang X, Huang ZG, Yue TM (2002) Experimental investigation into shaping particles-reinforce material by WEDM HS. J Mater Process Technol 129:56 – 59.*

7. *Yan BH, Tsai HC (2005) Examination of wire electrical discharge machining of Al_2O_3/6061Al composites. Int J Mach Tools Manuf 45(3):251 – 259.*

8. *Aniza Alias, Bulan Abdullah, Norliana Mohd Abbas, Influence of machine feed rate in wedm of titanium Ti-6Al-4V with constant current (6a) using brass wire, Procedia Engineering, 41, (2012), 1806 – 1811.*

9. *Kodalagara Puttanarasaiah Somashekhar & Nottath Ramachandran & Jose Mathew, Material removal characteristics of microslot (kerf) geometry in μ-WEDM on aluminium Int J Adv Manuf Technololgy, 2010, 51:611–626.*

10. *Sangju Lee, Michael A. Scarpulla, Eberhard Bamberg, Effect of metal coating on machinability of high purity germanium using wire electrical discharge machining, Journal of Materials Processing Technology 213 (2013) 811–817*

11. *Nihat Tosun, Can Cogun and Gul Tosun, 2004, A study on kerf and material removal rate in wire electrical discharge machining based on Taguchi method, Journal of Materials Processing Technology – Journal of material processing and technology, vol. 152, no. 3, pp. 316-322, 2004.*

12. *K. Palanikumar, R. Karthikeyan, Optimal machining conditions for turning of particulate metal matrix composites using Taguchi and response surface methodologies, Machining Science and Technology: An International Journal, 10:417–433.*

13. *Montgomery, D. C., "Design and analysis of experiments", 5th edition, John Wiley & Sons, INC, New York, 2003.*

14. *Chen CJ, Tseng CS (1996) The path and location planning of workpiece by genetic algorithms. J Intell Manuf 7:69*

15. *Dereli T, Filiz IH, Baykasoglu A (2001) Optimizing cutting parameters in process planning of prismatic parts using genetic algorithms. Int J Prod Res 39:3303*

16. *P. Palanisamy, I. Rajendran, S. Shanmugasundaram, Optimization of machining parameters using genetic algorithm and experimental validation for end-milling operations, International Journal of Advanced Manufacturing Technology, 32: (2007) 644 – 655.*

17. *Kalyanmoy Deb, Optimization for engineering design : Algorithms and Examples, PHI Learning Limited, New Delhi, 2010.*

18. *Deb, K., "Multi objective optimization using evolutionary algorithms", John Wiley & Sons (ASIA) Pte. Ltd., Singapore, 2001.*

Appendix A

Table 7: Crossover and Mutation in GA (Minimization of Kw)

Selection	Mating pool	Cross over?	Cross -over site	Offspring	Mutation sites	Mutated chromosome
6	11010 1001 0010 000 010	NO	--	11010 1001 0010 000 010	--	11010 1001 0010 000 010
20	11000 1100 0011 111 001	NO	--	11000 1100 0011 111 001	8	11000 1110 0011 111 001
9	10011 0000 1101 010 111	NO	--	10011 0000 1101 010 111	--	10011 0000 1101 010 111
10	10001 1101 0011 110 011	NO	--	10001 1101 0011 110 011	--	10001 1101 0011 110 011
24	10011 1100 1011 011 011	YES	9,16	10011 1100 0011 111 011	--	10011 1100 0011 111 011
13	10101 1101 0011 111 101	YES	9,16	10101 1101 1011 011 101	--	10101 1101 1011 011 101
8	01111 1111 1000 001 101	NO	--	01111 1111 1000 001 101	2,10	00111 1111 0000 001 101
2	10111 1101 0011 011 000	NO	--	10111 1101 0011 011 000	--	10111 1101 0011 011 000
1	10011 1111 1101 000 111	NO	--	10011 1111 1101 000 111	--	10011 1111 1101 000 111
18	10101 1010 1010 000 111	NO	--	10101 1010 1010 000 111	--	10101 1010 1010 000 111
17	11001 0011 1100 101 010	NO	--	11001 0011 1100 101 010	--	11001 0011 1100 101 010
2	10111 1101 0011 011 000	YES	5,9	10111 1111 0011 011 000	5	10110 1111 0011 011 000
1	10011 1111 1101 000 111	YES	5,9	10011 1101 1101 000 111	--	10011 1101 1101 000 111
24	10011 1100 1011 011 011	NO	--	10011 1100 1011 011 011	--	10011 1100 1011 011 011
15	11001 1100 1100 011 001	NO	--	11001 1100 1100 011 001	7,3	11101 1000 1100 011 001
23	11011 0101 0011 101 011	NO	--	11011 0101 0011 101 011	--	11011 0101 0011 101 011
20	11000 1100 0011 111 001	NO	--	11000 1100 0011 111 001	--	11000 1100 0011 111 001
8	01111 1111 1000 001 101	NO	--	01111 1111 1000 001 101	--	01111 1111 1000 001 101
23	11011 0101 0011 101 011	NO	--	11011 0101 0011 101 011	--	11011 0101 0011 101 011
24	10011 1100 1011 011 011	YES	9,13	10011 1100 0101 011 011	--	10011 1100 0101 011 011
4	11001 0110 0101 000 001	YES	9,13	11001 0110 1011 000 001	8,15	11001 0100 1011 010 001
11	10100 0110 0101 001 101	NO	--	10100 0110 0101 001 101	--	10100 0110 0101 001 101
25	00100 0010 0010 110 001	NO	--	00100 0010 0010 110 001	--	00100 0010 0010 110 001
14	11111 0111 0001 000 111	NO	--	11111 0111 0001 000 111	--	11111 0111 0001 000 111
11	10100 0110 0101 001 101	NO	--	10100 0110 0101 001 101	--	10100 0110 0101 001 101
7	11101 1011 0110 100 001	NO	--	11101 1011 0110 100 001	--	11101 1011 0110 100 001
1	10011 1111 1101 000 111	NO	--	10011 1111 1101 000 111	--	10011 1111 1101 000 111

Appendix B

Table 9: Validation of Results for Kw

Exp. No.	Machining conditions					Kw (mm)		
	Size of SiC_P (μs)	Volume of SiC_P (%)	Pulse-on time (μs)	Pulse-off time (μs)	Wire tension (gm)	Predicted	Experiment	Deviation (%)
1	25	7	5	29	1	0.3011	0.3012	0.03470
2	50	10	8	26	6	0.3398	0.3398	0.00523
3	75	13	9	42	3	0.3162	0.3163	0.02880
4	50	8	6	30	6	0.3244	0.3246	0.06165
5	75	11	7	40	3	0.3091	0.3101	0.32351
6	25	13	8	38	7	0.3372	0.3393	0.61196
7	75	15	9	35	9	0.3149	0.3150	0.04132
8	25	3	7	37	5	0.3697	0.3705	0.21755
9	50	6	7	39	3	0.3336	0.3336	0.00000
10	25	5	6	27	6	0.3471	0.3486	0.42943
11	75	9	7	41	9	0.3198	0.3184	0.44530
12	50	12	9	42	7	0.3298	0.3299	0.03033
13	25	10	5	32	4	0.3065	0.3085	0.65260
14	50	14	6	37	3	0.3025	0.3026	0.03205
15	75	15	5	35	5	0.2939	0.2959	0.68043
16	25	8	8	38	8	0.3618	0.3619	0.02223
17	75	9	7	25	4	0.3193	0.3195	0.06263
18	50	6	6	30	2	0.3166	0.3168	0.06317

